University of New Orleans

ScholarWorks@UNO

Synthesis and characterization of nanocrystalline zinc ferrite

Gabriel Caruntu
University of New Orleans, gcaruntu@uno.edu

Charles J. O'Connor
University of New Orleans, coconnor@uno.edu

Follow this and additional works at: https://scholarworks.uno.edu/chem_facpubs

Part of the Chemistry Commons

Recommended Citation

Gabriel Caruntu, Gary G. Bush and Charles J. O'Connor. 2004. "Synthesis and characterization of nanocrystalline zinc ferrite." Journal of Materials Chemistry 14: 2753-2759.

Synthesis and characterization of nanocrystalline zinc ferrite films prepared by liquid phase deposition

Gabriel Caruntu,*[a] Gary G. Bush[b] and Charles J. O'Connor*[a]

[a]Advanced Materials Research Institute, Chemistry Department, University of New Orleans, New Orleans, LA, USA. E-mail: gcaruntu@uno.edu; coconnor@uno.edu
[b]Research & Development Division, Lockheed Missiles and Spacer Co., Palo Alto, CA, USA

We report on the synthesis of highly uniform, single phase zinc ferrite films prepared through a single step low temperature reaction by the liquid phase deposition (LPD) method. X-ray diffraction, TGA and EDX measurements support the assumption that the as-deposited films are constituted from a mixture of crystallized FeOOH and amorphous $Zn(OH)_2$. Upon heat treatment in air at 600 °C for one hour the intermediates are subsequently converted into the corresponding zinc ferrites. The films with adjustable chemical compositions are identified as having a spinel-type crystal structure and present a spherical or rod-like microstructure, depending on the Zn content. The magnetic films present a superparamagnetic behavior above blocking temperatures which decrease with increasing Zn content, and are ferromagnetic at 5 K with coercivities ranging between 797.8 and 948.5 Oe.

1. Introduction

Transition metal ferrites MFe_2O_4 represent an important class of technological materials, due to their remarkable properties which render them suitable for many applications in the next generation of electronics, catalysis and magnetic information storage. Although ferrites are traditionally prepared in bulk, the miniaturization of magnetic and electronic devices has demanded advanced materials with new forms and shapes, such as nanoparticles or thin films. Ferrite thin films can typically be deposited onto various substrates by various synthetic techniques which can be categorized into physical and chemical methods. Physical methods include molecular beam epitaxy,[1,2] magnetron sputtering[3,4] or pulse laser deposition (PLD)[5,6] whereas chemical processes include chemical vapor deposition (CVD),[7,8] electrodeposition,[9] electroless deposition,[10] hydrothermal,[11] spin spraying,[12,13] dip coating[14] and spin coating of sol–gel reagents.[15,16]

Although these methods allow for the preparation of ferrite films tailorable to particular applications, in most cases they present several critical shortcomings, *i.e.*, the need for expensive and sophisticated equipment to create a vacuum or a low pressure atmosphere, the thickness of the films cannot be controlled accurately during deposition, the line-of-sight deposition has limitations and films are often difficult to deposit onto surfaces with large areas or complex morphologies. The development of new synthetic strategies for the selective deposition of multicomponent oxide films is important for the future of microelectronic circuitry. Recently, a novel chemical method, called liquid phase deposition (LPD), has been proposed by Nagayama and co-workers[17] for the synthesis of metal oxide thin films. It consists of the direct precipitation of homogenous metal oxide films *via* the controlled hydrolysis of the corresponding solutions of transition metal–fluoro complexes in the presence of aluminum or boric acid (eqn. (1)). Control over the hydrolysis process is necessary in order to prevent spontaneous bulk precipitation of the solution.

$$MF_n^{(n-2m)-} + mH_2O \rightleftharpoons MO_m + nF^- + 2mH^+ \quad (1)$$

Boric acid or aluminum acts as a scavenger for the fluoride ions by forming the stable $[BF_4]^-$ ion (eqn. (2)), which causes the equilibrium reaction (eqn. (1)) to proceed to the right-hand side with formation of the metal oxide.

$$H_3BO_3 + 4HF \rightleftharpoons BF_4^- + H_3O^+ + 2H_2O \quad (2)$$
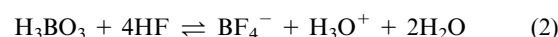
Initially developed for SiO_2[18] and TiO_2[19] films, the liquid phase deposition (LPD) method has rapidly been extended to other transition metal oxides (V, Cr, Mn, Fe, Co, Ni, In, Nb, Cu, Zn),[20–24] FeOOH and α-Fe_2O_3,[25] and Au-dispersed TiO_2 films,[26] respectively. Because the main process involved is a homogenous nucleation from aqueous solutions, liquid phase deposition harbors great promise for the fabrication of multicomponent metal oxide films. However, extension of the liquid phase deposition method to other oxide systems seemed to be limited, mainly due to the optimization of reaction conditions so that both transition metals can be rendered hydrolysable simultaneously, which often results in the failure of the chemical reaction.

Consequently, considerably less is known on the use of the liquid phase deposition method to synthesize single phase multicomponent oxide films. Gao and co-workers deposited polycrystalline perovskite-type ABO_3 (A = Sr, Ba) thin films with a columnar morphology,[27] whereas Deki and co-workers reported the formation of iron–nickel binary oxide films.[28] However, the prepared nickel ferrite samples show very poor crystallinity upon annealing at high temperature; in addition, the mechanism of formation of ferrites is not very well elucidated. To our knowledge, there are no other reports on the deposition of ferrite films by this soft solution process. The present investigation aims at the extension of the liquid phase deposition method to the preparation of nanocrystalline ferrite thin films. We report here our initial, successful attempts in developing the liquid phase deposition method for the synthesis of zinc ferrite films with different chemical compositions.

2. Experimental

2.1 Preparation of zinc ferrite films by chemical deposition

The experiments were performed in the open atmosphere using a magnetic hotplate with an external temperature controller. Source chemicals were reagent grade purity and used as received from Alfa Aesar. Deionized water (18 MΩ) was

obtained from a Barnstead Nanopure water purification system. Scheme 1 shows the details of the synthetic strategy used to deposit zinc ferrite films by the liquid deposition method. Prior to deposition, the substrates were degreased by washing repeatedly with acetone and then sonicated in MilliQ water. The parent solution was obtained by dissolving 0.25 g of FeO(OH) in 50 ml of 1 M $NH_4F \cdot HF$ aqueous solution. FeOOH was precipitated from an aqueous solution of $Fe(NO_3)_3 \cdot 7H_2O$ upon addition of a diluted solution of ammonia. The precipitate was then filtered, washed several times with distilled water and allowed to dry at room temperature in the open air for several days. Then, a separate aqueous solution of Zn^{2+} with a concentration of 2 M was prepared by dissolving the corresponding amount of zinc nitrate $Zn(NO_3)_2 \cdot 4H_2O$ in distilled water. Zinc ferrite thin films were deposited on non-alkali glass plates (Corning no. 7059) substrates and p-type {111} single crystal Si wafers, respectively. Three separate solutions of iron hydroxides, $Zn(NO_3)_2$ and boric acid (aqueous solution $c = 0.5$ M) were mixed in different proportions to obtain a final solution with fixed concentrations of iron and H_3BO_3, whereas the concentration of Zn^{2+} was varied in the range 10^{-3} to 5.5×10^{-1} M. Substrates were suspended vertically and soaked in the reaction solution at different temperatures ranging between 25 °C and 65 °C for different periods of time, typically ranging between 3 and 24 h. After being removed from the reaction solution, the films were carefully rinsed with distilled water, then sonicated and dried in the open atmosphere. To ensure complete crystallization of the zinc ferrite films, samples were subjected to heat treatment in the open air at 600 °C followed by natural cooling to room atmosphere.

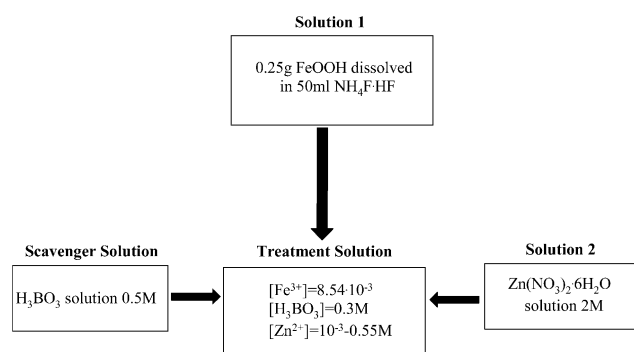### 2.2 Characterization of zinc ferrite films

The surface morphology and microstructure of the films was studied by using a JEOL-JSM 5410 scanning electron microscope, whereas their thicknesses were measured by a surface profile measuring system Dektak-IIA. Identification of the crystalline phases, crystallite size and the phase purity of the films were examined by X-ray diffraction using a Philips X'Pert System equipped with a curved graphite single-crystal mono-chromator (CuK_α radiation). Patterns were recorded in a step scanning mode in the 20–95° 2θ range with a step of 0.02° and a counting time of 10 s. The metal contents of the deposited zinc ferrite films were determined by inductive coupled plasma (ICP) spectroscopy, using a Varian FT220 s flame absorption spectrometer. The resonance wavelengths were $\lambda_{(Fe)} = 234.35$, 238.204 and 259.94 nm, and $\lambda_{(Zn)} = 202.548$, 206.2 and 213.86 nm, respectively. The correlation coefficient used to calibrate the instrument was 0.999147 and the calibration error did not exceed 5%. The corresponding solutions were prepared by dissolving the films in 18% HCl and then diluting them to the required concentrations. Examination of the thermal behavior of the as-grown films was performed using a TA

Instrument TGA 2950. Approximately 5 mg of powdered sample were heated under a flow of air (flow rate 25 ml min^{-1}) from room temperature to 600 °C in an alumina crucible. Infrared spectra were collected with a Nicolet Magna 750 FTIR instrument. Samples were prepared by mixing the ferrite powders obtained by scratching the films with KBr and then forming them into pellets. Spectra were recorded over the range of $\lambda = 4000$ to 500 cm^{-1} with a resolution of 5 cm^{-1}. Magnetic properties were investigated with a Quantum Design MPMS-5S SQUID magnetometer.

3. Results and discussion

A low temperature, single step deposition of solutions of transition metal salts in $NH_4F \cdot HF$ led to highly uniform, well-adhering zinc ferrite films with a thickness which could be easily controlled by varying the deposition time. During the course of the deposition process, the initial colorless treatment solution turned slowly to a brownish colloidal suspension which became progressively clear and colorless as the chemical deposition of the films was achieved. The pH of the solution slightly increased from 4–5 to 6, which is presumably ascribed to the formation of basic transition-metal oxides/oxyhydroxides as a result of the simultaneous hydrolysis of the corresponding salts. Additionally, an amorphous fine brown powder was detected at the bottom of the reaction vessel as well as a thin light brown film on its walls. Therefore, this clearly indicates that films form through attachment of primarily fine particles of transition metal oxides/hydroxides which are originally precipitated in the bulk solution as a result of the hydrolysis of the transition-metal oxyfluoro-complexes. In Fig. 1(a) is shown the evolution of the Zn/Fe ratio of the deposited ferrite films (obtained from ICP measurements) with increasing zinc concentration in the treatment solution. The elemental analysis performed by EDX has shown that the films are fluorine free and chemically homogenous through the whole surface. Additionally, the composition of films deposited after 2, 4, 6, 12 and 24 hours did not reveal major differences in the Zn/Fe ratio, which indicates that the chemical composition does not vary during the deposition process. Fig. 1(a) reveals the existence of two growth regimes, that is, for initial concentrations of Zn^{2+} ranging between 10^{-3} and 10^{-2} M the curve shows a logarithmic character, whereas when $[Zn^{2+}] > 0.1$ M it becomes linear. This trend is consistent with that observed for the variation of the Zn/Fe ratio with the Zn content of the treatment solution (Fig. 1(c)) suggesting that the composition of the film is solely dictated by the Zn/Fe ratio of the treatment solution. Assuming a stoichiometric Fe/O ratio in the prepared ferrites, the corresponding film composition as determined by ICP spectroscopy is indicated in Table 1. The error in measuring the elemental composition of the films was less than 5%. As expected, the Zn content of the deposited films increases progressively with increasing the Zn^{2+} concentration in the treatment solution. Ferrite films with highly tunable chemical composition can be obtained by liquid phase deposition by simply controlling the volumes of transition metal salts in the treatment solution. This is important since mastery of the chemical composition of ferrite films has proven to be critical for further technological applications.

In addition to the concentration of the initial solutions, temperature was found to play an important role in the kinetics of ferrite deposition. For a given deposition time, an increase in the reaction temperature accelerates the chemical deposition which in turn results in thicker films. However, when the reaction was performed at room temperature, no precipitate was observed even after 3 days. As shown in Fig. 2, the film thickness varies roughly linearly with the deposition time and was found to range typically between 50 and 960 nm for a deposition time of 2–24 hours, depending on the temperature.

Solution 1

0.25g FeOOH dissolved in 50ml $NH_4F \cdot HF$

Scavenger Solution

H_3BO_3 solution 0.5M

Treatment Solution

$[Fe^{3+}]=8.54 \cdot 10^{-3}$ $[H_3BO_3]=0.3M$ $[Zn^{2+}]=10^{-3}-0.55M$

Solution 2

$Zn(NO_3)_2 \cdot 6H_2O$ solution 2M

Scheme 1 Synthetic strategy used to deposit zinc ferrite films by the liquid phase deposition (LPD) method.
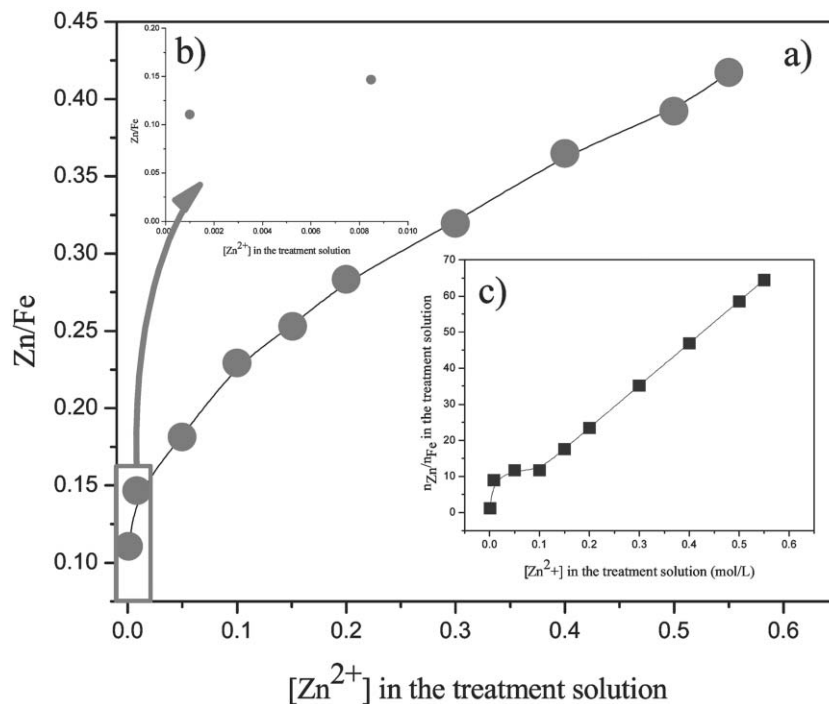
Fig. 1 (a) Variation of the Zn/Fe ratio of the film with the Zn^{2+} concentration of the reaction solution; (b) close-up of Fig. 1(a) in the concentration range 10^{-3}–10^{-2} M; (c) variation of the Zn/Fe ratio in the treatment solution with the concentration of Zn^{2+} ion.

Table 1 Film composition obtained from ICP measurements

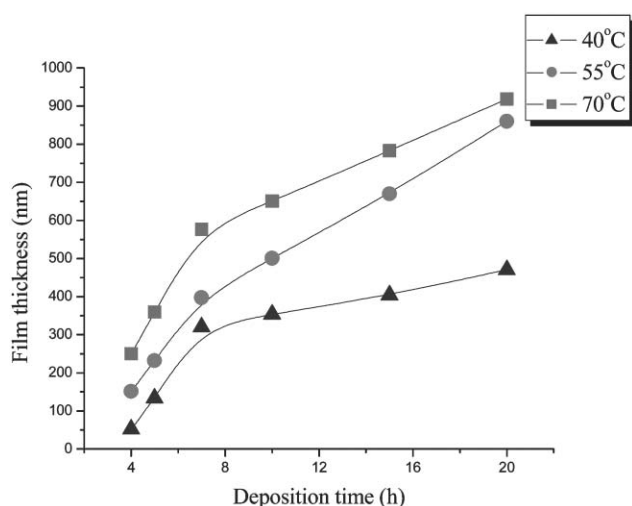| $[Zn^{2+}]$ in the starting solution (mol l^{-1})	10^{-3}	8.54×10^{-3}	0.1	0.2	0.3	0.4	0.5	0.55
Film composition	$Zn_{0.31}Fe_{2.69}O_4$	$Zn_{0.38}Fe_{2.62}O_4$	$Zn_{0.56}Fe_{2.44}O_4$	$Zn_{0.66}Fe_{2.34}O_4$	$Zn_{0.73}Fe_{2.27}O_4$	$Zn_{0.81}Fe_{2.19}O_4$	$Zn_{0.84}Fe_{2.16}O_4$	$Zn_{0.88}Fe_{2.12}O_4$

Fig. 2 Dependence of the film thicknesses on the deposition time at different reaction temperatures.

Although the mechanism seems to be complex, the slight change of the slope observed after 7 hours is attributed to the kinetics of the deposition process. Because the solutions of transition metal oxides/hydroxides resulting from hydrolysis are supersaturated, their ionic products (IP) largely exceed the corresponding solubility product (SP). Consequently, precipitation occurs faster in the first stage of the deposition process (induction period) and is progressively inhibited as the deposition progresses and, correspondingly, the ionic product approaches the solubility product of the solution.

The X-ray diffraction patterns of the as-deposited ferrite films show that they are composed of well crystallized

FeO(OH). It is important to note that the composition of the as-deposited films is very sensitive to the reaction conditions. When ordinary distilled water is used to prepare the reaction solutions, akaganeite FeO(OH, Cl) (JCPDS 13–157) was deposited instead of β-lepidocrocite FeO(OH) (JCPDS 08–0098) which is obtained when using MilliQ water. Although any zinc-containing crystalline phase was detected by X-ray diffraction, EDX experiments revealed the presence of Zn in the as-deposited films with a Fe/Zn ratio in good agreement with the results obtained from ICP spectroscopy. Because it was not detected by X-ray diffraction, but observed by ICP measurements, zinc is presumably present in the as-prepared films as an amorphous $Zn(OH)_2$ phase. Fig. 3 displays the TG thermogram of the sample with the composition $Zn_{0.81}Fe_{2.19}O_4$ at a heating rate of 1 °C min^{-1} under flowing air. The mass loss profile exhibits a very well defined decrease over the temperature range 25–600 °C, which corresponds to the two step conversion of the intermediates into the final products.

The first inflection point observed at $T \approx 150$ °C (weight loss $\approx 7\%$) is associated with the loss of the hydrated and lattice water, whereas the second one observed at $T \approx 460$ °C (weight loss 25.57%) is associated to a dehydroxylation reaction of the appropriate ratios of transition metal hydroxides: $2OH^- \rightarrow O^{2-} + H_2O$ ($FeOOH \rightarrow \frac{1}{2}Fe_2O_3 + \frac{1}{2}H_2O$, weight loss 14.516%; and $Zn(OH)_2 \rightarrow ZnO + H_2O$, weight loss 11.1465%) followed by the partial reduction of the Fe^{3+} ions to Fe^{2+} (weight loss 0.997%). The mass variation deduced from considering the as-deposited film as a mixture of FeOOH and $Zn(OH)_2$ in a ratio given by the Zn/Fe ratio obtained from ICP spectroscopy is in excellent agreement with the mass loss observed from the TGA curve. Such a result corroborates the assumption that the as-grown films contain $Zn(OH)_2$, which is presumably amorphous since is not detected by X-ray
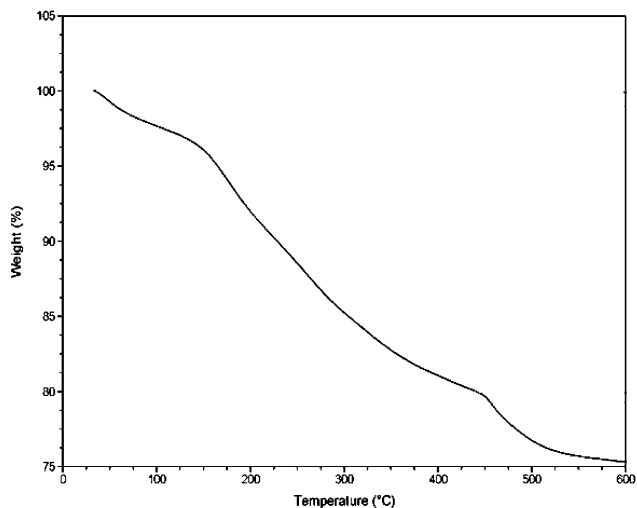
Fig. 3 Thermogravimetric analysis (TG) of hydroxide intermediates with a heating rate of 1 °C min^{-1}.
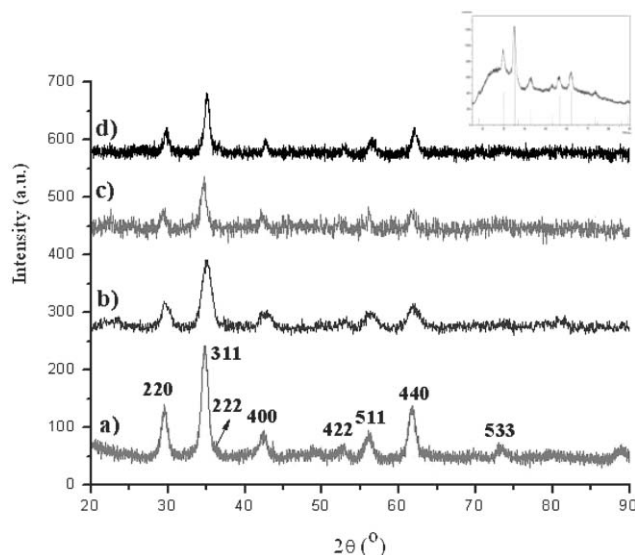

Fig. 4 Typical X-ray diffraction patterns of the annealed films obtained from the reaction solutions with initial Zn^{2+} concentrations of: (a) 0.1 M, (b) 0.2 M, (c) 0.4 M and (d) 0.5 M. The inset shows the raw XRD pattern of sample (a) without background subtraction.

diffraction. As shown in Fig. 4, the X-ray diffraction patterns of the annealed films were found to be similar for samples corresponding to different concentrations of Zn^{2+} in the starting solution. Accordingly, the relative intensities of the peaks indicate that the films do not present preferred orientation growth. In all cases, a broad pattern originating from the substrate dominated the experimental diffraction peaks. Background subtraction was performed by using the PowderX suite of programs.[29] All the experimental reflections are assigned to those of the standard polycrystalline $ZnFe_2O_4$ (franklinite, JCPDS 22–1012), which clearly indicates the formation of a spinel-type structure. The refined value of the cell parameter calculated for the film with the chemical composition $Zn_{0.84}Fe_{2.16}O_4$ was a = 8.449(3) Å, which is in good agreement with that of the standard bulk zinc ferrite (a = 8.4411 Å).[30] The crystallite size of the film was determined from the modified Scherrer formula,[31] which gives a mean crystallite size of 20 nm. In Fig. 5 are shown typical SEM micrographs of

the films deposited after 6 h, obtained from starting solutions with concentrations of Zn^{2+} ions ranging from 0 to 0.5 M.

As revealed in Fig. 5(a), in the absence of Zn^{2+} in the reaction solution, a uniform film of α-Fe_2O_3 is observed after the heat treatment. This film is composed of spherically shaped densely packed particles with a mean diameter of 200 nm, a value which is in good agreement to those previously reported by Deki and co-workers for β-FeO(OH)/α-Fe_2O_3 films obtained by the same synthetic approach.[25] In Fig. 5(b)–(f) are presented the SEM micrographs of the as-prepared and heat treated ferrite films, respectively.

Highly homogeneous films with a columnar architecture are observed in all cases, except the reaction solution whose zinc concentration is 0.1 M, where the particles forming the film
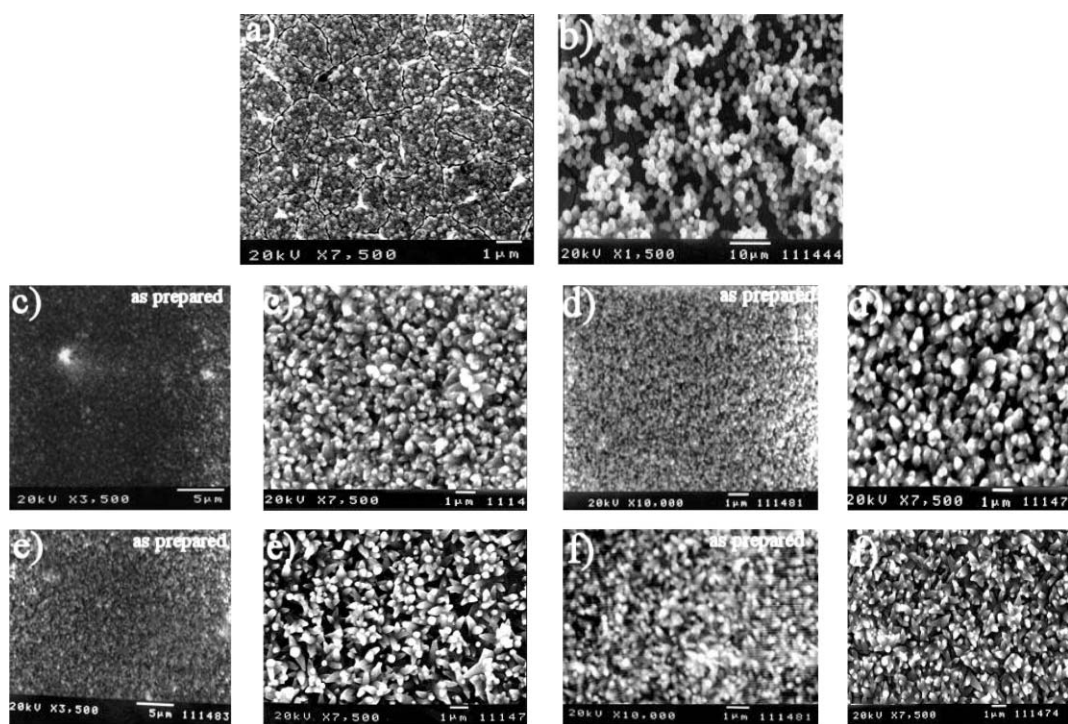

Fig. 5 Top-down SEM micrographs of zinc ferrite films deposited onto a Corning glass substrate from starting solutions with different Zn^{2+} concentrations: (a) 0 M, (b) 0.1 M, (c) 0.2 M, (d) 0.3 M, (e) 0.4 M and (f) 0.5 M. Micrographs (a) and (b) show annealed films, whereas micrographs (c)–(f) show both the as-deposited film and the annealed films, respectively

retain the spherical shape similar to that observed in the case of the α-Fe₂O₃ film. Although there is not clear evidence about the role played by Zn^{2+} ions on the morphology of the resulting films, experimental data show that the increase in the Zn^{2+} concentration is accompanied by a change of the morphology of the deposited films from a spherical to a rod-like type. Additionally, as in most cases reported for the liquid-phase deposition-based processing of thin films, it seems that deposition proceeds through heterogeneous nucleation of primary particles in solution followed by surface-directed growth.[32,33] In the other cases, films are constructed from large arrays of well defined rod-like particles of diameter 250–320 nm, grown perpendicularly to the substrate surface. The diameter of the nanorods doesn't vary noticeably with the concentration of Zn^{2+} in the reaction solution, but it is found to be influenced by the reaction time. A detailed investigation on the influence of the deposition time on the morphology of the films is currently being pursued and will be reported elsewhere. Additionally, we do not observe significant differences in the microstructure of the films before and after the thermal treatment, although the annealing in air at 600 °C results not only in the densification of ferrite films, but also in crystallization and grain growth. In order to fully treat the problem of chemical species involved in the deposition process, we performed UV-VIS spectroscopy measurements of the Fe^{3+} and Zn^{2+} solutions dissolved in water and an aqueous solution of 1 M NH₄F·HF. The UV-VIS spectrum in Fig. 6 shows that regardless of the solvent the Zn^{2+} solutions absorb visible radiation at the same wavelength (303 nm), whereas in the case of Fe^{2+} solutions, a different behavior is observed.

When water is replaced with an aqueous solution of 1 M NH₄F·HF the absorption band at 296 nm is substantially shifted to 338 nm. Such a shift indicates that the two transition metals in an aqueous solution of NH₄F·HF exist as differently coordinated species, that is, Fe^{3+} forms an oxyfluoro-complex $[FeF_6]^{3-}$ which further undergoes hydrolysis to give $[FeF_{6-x}(OH)_x]^{3-}$ anionic species, whereas Zn^{2+} ions are mainly coordinated by water molecules $[Zn(H_2O)_6]^{2+}$. These experimental observations are in agreement with the chemical character of the two Fe^{3+} ions pointed out by Arhland and co-workers;[34] their vacant d orbitals are "class a acceptors", which form stable complexes with anions favoring electrostatic bonding (F^-), whereas Zn^{2+} ions, with fully occupied d orbitals, show much more "class b-type" characteristics with respect to anion complexation. Consequently, coordination with anions possessing lone pairs of electrons like O^{2-} will be favored, explaining why zinc is not known to form stable fluoro-complexes in aqueous solutions.[35]

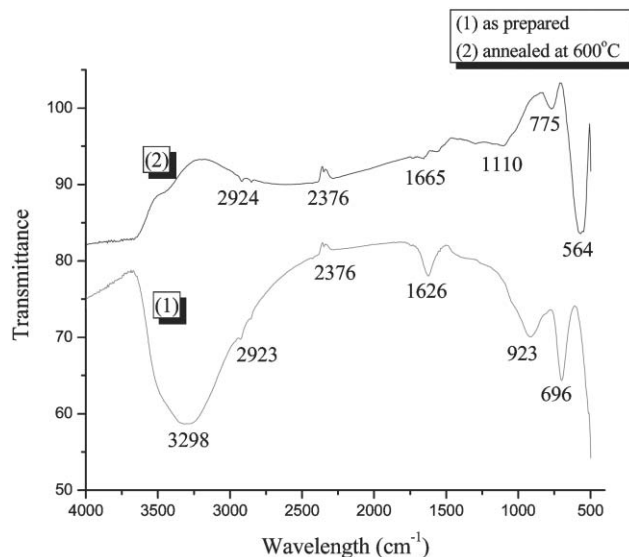The IR spectrum of the annealed ferrite film with chemical

Fig. 7 Infrared spectra of a $Zn_{0.81}Fe_{2.19}O_4$ film.

composition of $Zn_{0.82}Fe_{2.18}O_4$ (Fig. 7) exhibits typical absorption bands for the spinel structure, located at 564 cm⁻¹ and 775 cm⁻¹. These bands are accounted for by the stretching vibrations produced by the interaction of the metal ions in the tetrahedral and octahedral sites with oxygen.[36] Additionally, we observe that the bands of the annealed sample are shifted with respect to those observed for the as-prepared sample, which is attributable to the conversion of the hydroxide intermediates into the spinel structure as well as to the increase in crystallinity of the film.[37] The presence of a band at 2376 cm⁻¹ is due to atmospheric CO_2, which has been adsorbed on the surface of the powder during the preparation of the pellets. The absorption bands detected at 3298 cm⁻¹, 1626 cm⁻¹ and 923 cm⁻¹ in the case of the as-grown sample are ascribed to water (stretching mode) and the stretching and in-plane bending modes of the surface absorbed OH groups, respectively, which vanish upon heat treatment.[38] Zinc ferrite films were characterized by using standard zero-field-cooling (ZFC) and field-cooling (FC) procedures. The temperature dependence of the magnetization was measured between 5 K and 300 K under an external static magnetic field of 100 Oe, as shown in Fig. 8. Coercivity was measured at low temperature for each sample, whereas at room temperature no hysteresis was detected. The magnetic behavior observed experimentally is typical for all the samples investigated, with small variations of the values of the saturation magnetization and coercivity. We observe that the
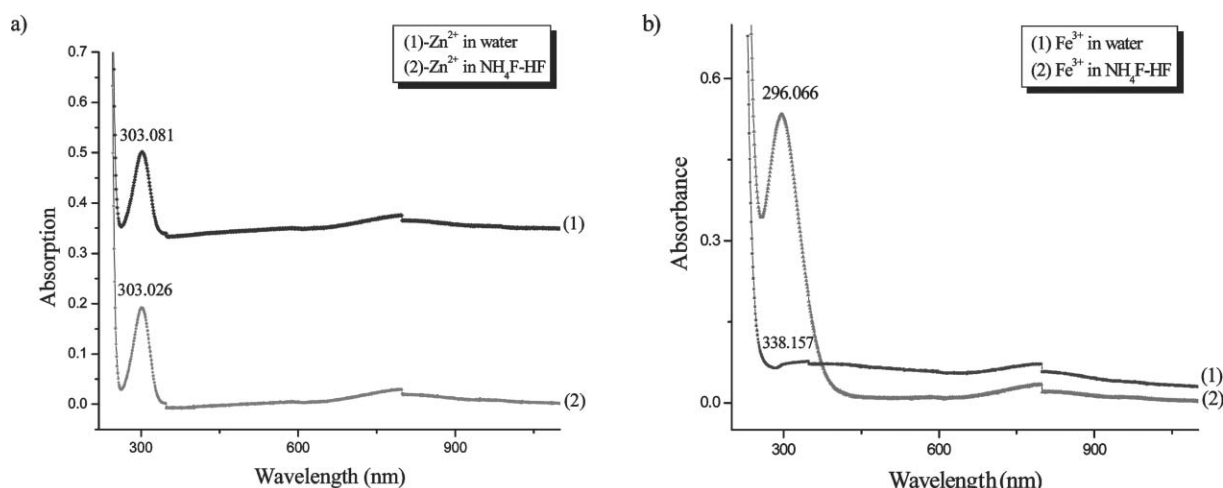

Fig. 6 UV-VIS spectra of Fe^{3+} and Zn^{2+} ions dissolved in water and an aqueous solution of NH₄F·HF (1 M)

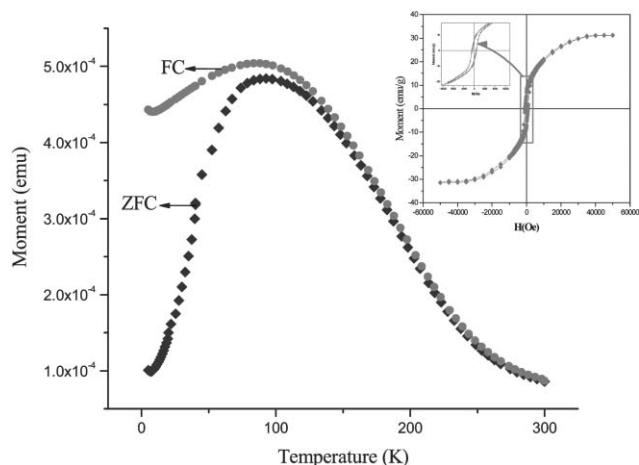**Fig. 8** ZFC and FC curves for a $Zn_{0.73}Fe_{2.27}O_4$ film. The inset shows the hysteresis loop recorded at 5 K.

ZFC and FC data diverge at low temperature, which is specific to superparamagnetic behavior of the zinc ferrite films.

Table 2 summarizes the blocking temperatures, the values of the saturation magnetization and the coercivities, measured at 5 K. The blocking temperature and saturation magnetization roughly decrease with increasing the zinc composition of the sample. Below the critical temperature T_c, the samples exhibit a ferrimagnetic behavior, which is related to the cationic disorder of the two sublattices (denoted by A for tetrahedral and B for octahedral) of the spinel structure. The coercivity is found to increase with increasing the Zn content of the films, whereas the values of the magnetization saturation fall within the range reported in literature for zinc ferrites.[39] However, the saturation magnetization is much lower than is the case for $ZnFe_2O_4$ films obtained by rf sputtering, whose magnetization at 5 K was reported to be 90 emu g^{-1} for a cation distribution given by the formula $(Zn_{0.4}Fe_{0.6})^{tet}(Zn_{0.6}Fe_{1.4})^{oct}O_4$.[40] Such a low value for the saturation magnetization originates from a much smaller fraction of Fe^{2+} ions distributed over the tetrahedral sites which gives rise to a net magnetic moment of the tetrahedral sublattice and, in turn, enhances the A–B interactions at the expense of the B–B ones.

4. Conclusions

Liquid phase deposition offers a simple, feasible, non-toxic and easily scalable aqueous low temperature route to the synthesis of single phase ferrite thin films. Highly homogeneous films have a chemical composition which can be easily controlled through tailoring the concentration of metal ions in the reaction solution. Zinc ferrite films present a complex morphology, being constructed from particles with spherical or rod-like shapes, which seem to be influenced to a certain extent by the concentration of zinc ions in the reaction solution. UV-VIS measurements of the solution precursors have shown that precipitation of zinc ferrite films occurs *via* a complex OH^- bridged polynuclear complex, which is a result of the interaction between hydrolysed $[FeF_6]^{3-}$ and $[Zn(H_2O)_6]^{2+}$ species detected in the reaction solutions. The prepared Zn ferrite films show a superparamagnetic behavior with blocking temperatures ranging from 88 to 107 K. At 5 K the films have a ferrimagnetic behavior strongly influenced by the cationic

Table 2 Magnetization characteristics of the zinc ferrite films as a function of the zinc content

Zn/Fe atomic ratio	T_B/K	M_s/emu g^{-1}	H_c/Oe
0.327	107.5	32.11	943.6
0.369	88.65	28.68	948.5

distribution over the two crystallographic sites. The extension of the liquid phase deposition method to the preparation of other important transition metal ferrite films is currently being pursued and will be reported elsewhere.

Acknowledgements

References

1 T. Tsurumi, T. Suzuki, M. Yamaze and M. Daimon, *Jpn. J. Appl. Phys.*, 1994, **33**, 5192.
2 I. Wane, F. Cosset, A. Bessaudou, A. Celerier, C. Girault, J. L. Decossas and J. C. Vareille, EUROMAT 99, Biannual Meeting of the Federation of European Materials Societies (FEMS), Munich, Germany, Sept. 27–30, 1999, **vol. 9**, p. 54–61.
3 M. Tachiki, M. Noda, K. Yamada and T. Kobayashi, *J. Appl. Phys.*, 1998, **83**, 5351.
4 H. Y. Zhang, B. X. Gu, H. R. Zhai and M. Lu, *Phys. Status Solidi A*, 1994, **143**, 399.
5 D. Ravinder, K. V. Kumar and A. V. R. Reddy, *Mater. Lett.*, 2003, **57**, 4162.
6 P. C. Dorsey, P. Lubitz, D. B. Chrisey and J. S. Horwitz, *J. Appl. Phys.*, 1996, **79**(8), 6338.
7 P. A. Lane, P. J. Wright, M. J. Crosbie, A. D. Pitt, C. L. Reeves, B. Cockayne, A. C. Jones and T. J. Leedham, *J. Cryst. Growth*, 1998, **192**(3–4), 423.
8 H. Itoh, T. Uemura, H. Yamaguchi and S. Naka, *J. Mater. Sci*, 1989, **24**(10), 3549.
9 S. D. Sartale and C. D. Lokhande, *Ceram. Int.*, 2002, **28**(5), 467–477.
10 Surve Vandan and Puri Vijaya, *Bull. Electrochem.*, 1998, **14**(4–5), 151.
11 Shu-Hong Yu and Yoshimura Masahiro, *Chem. Mater.*, 2000, **12**(12), 3805.
12 M. Taheri, E. E. Carpenter, V. Cestone, M. M. Miller, M. P. Raphael, M. E. McHenry and V. G. Haris, *J. Appl. Phys.*, 2002, **91**(10), 7595.
13 N. Matsushita, C. P. Chong, T. Mizutani and M. Abe, *J. Appl. Phys.*, 2002, **91**(10), 7376.
14 J. G. dos S. Duque, M. A. Macedo, N. O. Moreno, J. L. Lopez and H. D. Pfanes, *J. Magn. Magn. Mater.*, 2001, **226–230**, 1424.
15 S. D. Sathaye, K. R. Patil, S. D. Kulkarni, P. P. Bakre, S. D. Pradhan, B. D. Sarwade and S. N. Shintre, *J. Mater. Sci.*, 2003, **38**(1), 29.
16 F. Cheng, Z. Peng, Z. C. Liao and C. Yan, *Thin Solid Films*, 1999, **339**, 109.
17 J. Ino, A. Hishinuma, H. Nagayama and H. Kawahara, *Jpn. Pat.* 01093443A (Nippon Sheet Glass), June 7, 1988.
18 H. Nagayama, H. Honda and H. Kawahara, *J. Electrochem. Soc.*, 1988, **135**, 2013.
19 S. Deki, Y. Aoi, O. Hiroi and A. Kajinami, *Chem. Lett.*, 1996, 433.
20 S. Deki, Y. Aoi, Y. Miyake, A. Gotoh and A. Kajinami, *Mater. Res. Bull.*, 1996, **31**(11), 1399.
21 K. Tsukuma, T. Akiyama and H. Imai, *J. Non-Cryst. Solids*, 1997, **210**, 48.
22 P. Pramanik and S. Bhattacharya, *J. Electrochem. Soc.*, 1990, **137**, 3869.
23 M. Izaki and T. Omi, *J. Electrochem. Soc.*, 1997, **144**, L3.
24 H. Ko, Y. Yu, M. Mizuhata, A. Kajinami and S. Deki, *J. Electroanal. Chem.*, 2003, **559**, 91.
25 S. Deki, Y. Aoi, J. Okibe, H. Yanagimoto, A. Kajinami and M. Mizuhata, *J. Mater. Chem.*, 1997, **7**, 1769.
26 S. Deki, Y. Aoi, H. Yanagimoto, K. Ishii, K. Akamatsu, M. Mizuhata and A. Kajinami, *J. Mater. Chem.*, 1996, **6**, 1879.
27 Y. Gao, Y. Masuda, T. Yinezawa and K. Koumoto, *Chem. Mater.*, 2002, **14**, 5006.
28 S. Deki and Y. Aoi, *J. Mater. Res.*, 1998, **13**(4), 883.
29 C. Dong, *J. Appl. Cryst.*, 1999, **32**, 838.
30 W. Schiessi, W. Potzel, H. Kartzel, M. Steiner, G. Kalvius, A. Martin, M. Krause, I. Halevy, J. Gal, W. Schafer, G. Will,

M. Hillberg and R. Wappling, *Phys. Rev. B: Condens. Mattter*, 1996, **53**, 9143.

31 H. P. Klug and L. E. Alexander, *X-Ray Diffraction Procedure for Polycrystalline and Amorphous Materials* (2nd Ed.), Wiley, New York, 1974.

32 K. Koumoto, S. Seo, T. Sugiyama and W. S. Seo, *Chem. Mater.*, 1999, **11**(9), 2305.

33 T. P. Niesen, J. Bill and F. Aldinger, *Chem. Mater.*, 2001, **13**, 1552.

34 S. Ahrland, J. Chatt and N. R. Davis, *Q. Rev., Chem. Soc.*, 1958, **12**, 265.

35 F. A. Cotton, G. Wilkinson, C. A. Murillo and M. Bochmann, *Advanced Inorganic Chemistry* (6th Ed.), John Wiley & Sons, New York, 1999.

36 M. Andres-Verges, C. de Julian, J. M. Gonzales and C. J. Serna, *J. Mater. Sci.*, 1993, **28**, 2962.

37 X. Li, G. Lu and S. Li, *J. Alloys Compd.*, 1996, **235**, 150.

38 M. Ishii, M. Nakanira and T. Yamanaka, *Solid State Commun.*, 1972, **11**, 209.

39 J. Smit and H. P. J. Wijn, *Ferrites*, Wiley, New York, 1959.

40 K. Tanaka, S. Nakashima, K. Fujita and K. Hirao, *J. Phys.: Condens. Matter*, 2003, **15**, L469.